Bifurcations of stable sets in noninvertible planar maps

J. P. England, B. Krauskopf & H. M. Osinga
Bristol Centre for Applied Nonlinear Mathematics
Department of Engineering Mathematics, University of Bristol,
Queen's Building, Bristol BS8 1TR, UK

June 2004

Keywords: Noninvertible map, stable set, critical curve, bifurcation, basin of attraction.

Abstract

Many applications give rise to systems that can be described by maps that do not have a unique inverse. We consider here the case of a planar noninvertible map. Such a map folds the phase plane, so that there are regions with different numbers of pre-images. The locus where the number of pre-images changes is made up of so-called critical curves, which are defined as the images of the locus where the Jacobian is singular. A typical critical curve corresponds to a fold under the map, so that the number of pre-images typically changes by two.

We consider the question of how the stable set of a hyperbolic saddle of a planar noninvertible map changes when a parameter is varied. The stable set is the generalization of the stable manifold for the case of an invertible map. Owing to the changing number of pre-images, the stable set of a noninvertible map may consist of finitely or even infinitely many disjoint branches. It is now possible to compute stable sets with the Search Circle algorithm that we developed recently.

We take a bifurcation theory point of view and consider the two basic codimension-one interactions of the stable set with a critical curve, which we call the outer-fold and the inner-fold bifurcations. By taking into account how the stable set is organized globally, these two bifurcations allow one to classify the different possible changes to the structure of a basin of attraction that are reported in the literature. The fundamental difference between the stable set and the unstable manifold is discussed. The results are motivated and illustrated with a single example of a two-parameter family of planar noninvertible maps.

1 Introduction

One often encounters maps arising in applications that are noninvertible, by which is meant that the given map is smooth, but does not have a uniquely defined inverse. A well-referenced example of such a noninvertible system is that of a discrete-time adaptive control system [Adomaitis *et al.*, 1991, Frouzakis *et al.*, 1992, Frouzakis *et al.*, 1996]. In this example one

finds multistability and the noninvertibility plays an important role in the structure of the basins of attraction of the coexisting attractors, which may consist of disconnected regions. Generally, knowledge of the structure of the basins of attraction is key to understanding the long term evolution of the system. Other applications that give rise to noninvertible maps include models from economics [Agliari, 2000, Agliari *et al.*, 2003], radiophysics [Maistrenko *et al.*, 1996] and neural networks [Rico-Martinez *et al.*, 2000].

In this paper we focus on noninvertible maps of the plane. That is, we consider a dynamical systems that is given by a smooth planar map

$$f : \mathbb{R}^2 \mapsto \mathbb{R}^2,$$

which does not have a unique inverse.

Geometrically such a noninvertible map folds the phase plane. Adopting the notation in [Nien and Wicklin, 1998] the *curve of merging pre-images* (also denoted LC_{-1}) is defined as

$$J_0 = \left\{ \mathbf{x} \in \mathbb{R}^2 \mid Df\left(\mathbf{x}\right) \text{is singular} \right\},$$

and the iterate of this curve, $J_1 = f(J_0)$, is called a *critical curve* (also denoted LC). The dynamics of a planar map is such that the phase plane folds along the critical curves. Generically, the number of pre-images of two points on either side of a fold line differs by two [Arnol′d, 1992], and points on the critical curve have two coincident pre-images. We focus on this generic case of a simple fold, such that points on one side of J_1 have two more pre-images than points on the other side. Common notation denotes Z_k as a region having k rank-one pre-images. The simplest case of a single fold is then denoted by (Z_0–Z_2), where points on one side of the fold have no pre-images and points on the other side of the fold have two pre-images. The folding of the phase plane may be more complicated, for example, for the case denoted (Z_1–Z_3–Z_1) there are regions with one and three pre-images.

Much work has been done to investigate the dynamics of noninvertible maps and how it is related with the folding of the phase plane [Abraham *et al.*, 1997, Gumowski and Mira, 1977, Gumowski and Mira, 1980a, Gumowski and Mira, 1980b, Mira *et al.*, 1996a, Mira *et al.*, 1996b]. In particular, there has been considerable interest in bifurcations that lead to qualitative changes of basins of attraction [Agliari *et al.*, 2003, Cathala, 1998, Kitajima *et al.*, 2000, López-Ruiz and Fournier-Prunaret, 2003, Mira *et al.*, 1994]. Such basins are typically determined by computing the orbits for a large number of initial conditions. An alternative is to compute the stable set of a suitable saddle point, which typically forms the boundary of a given basin of attraction.

To define the stable set formally, assume that f has a saddle fixed point $\mathbf{x}_0 = f(\mathbf{x}_0)$ and that f is differentiable in a neighborhood of $\mathbf{x}_0$. The global stable set $W^s(\mathbf{x}_0)$ of $\mathbf{x}_0$ is defined as the set of points that converge to $\mathbf{x}_0$ under forward iteration of f,

$$W^s(\mathbf{x}_0) = \left\{ \mathbf{x} \in \mathbb{R}^2 \mid f^n(\mathbf{x}) \to \mathbf{x}_0 \text{ as } n \to \infty \right\}.$$

For an invertible map $W^s(\mathbf{x}_0)$ is an embedded manifold and one speaks of $W^s(\mathbf{x}_0)$ as the stable manifold. However, when multiple inverses exist $W^s(\mathbf{x}_0)$ may consist of disjoint pieces. In particular, this set is not an embedded manifold and this is why one speaks of $W^s(\mathbf{x}_0)$ as the global stable set [Mira *et al.*, 1996b]. Throughout this paper, the *primary manifold* is the unique connected subset of $W^s(\mathbf{x}_0)$ that contains the fixed point $\mathbf{x}_0$.

The computation of stable sets and inverse orbits is difficult due to the fact that the Jacobian may become singular and that the critical curves separate the phase plane into regions that have different number of pre-images. Furthermore, the stable set may also consist of pieces that are disconnected from the saddle point. The recently developed Search Circle (SC) algorithm [England *et al.*, 2004] overcomes the problem of computing the primary manifold past intersections with the curve J_0 where the Jacobian is singular. It can also be used to compute disjoint pieces of the stable set. All that is needed to start a computation are the system equations themselves along with the saddle point and the stable eigenvector. All primary manifolds and stable sets in this paper have been computed with the implementation of the SC algorithm [Osinga and England, 2003] in the DsTool environment [Back *et al.*, 1992].

The SC algorithm makes it possible to find and consider codimension-one bifurcations where the stable set interacts with a critical curve. There are exactly two such codimension-one bifurcations, the outer-fold and inner-fold bifurcations that are discussed in detail in Sec. 3. (Similar interactions between unstable manifolds and attracting invariant circles have been investigated in [Frouzakis *et al.*, 1997, Frouzakis *et al.*, 2003, Maistrenko *et al.*, 1996].) Depending on the global organization of the stable set, these two basic codimension-one bifurcations may give rise to the different changes of basins of attraction that have been studied quite independently in the literature. This is discussed in Sec. 4. Finally, in Sec. 5 we illustrate the fundamental difference between the stable set and the unstable manifold. We discuss the codimension-one bifurcation that leads to structurally stable self-intersections of the unstable manifold, a phenomenon that cannot occur for the stable set.

2 Example

Throughout this paper we use a single example, namely the two-parameter family of planar noninvertible maps

$$Q\begin{pmatrix} x \\ y \end{pmatrix} = \begin{pmatrix} y \\ ax + bx^2 + y^2 \end{pmatrix}. \tag{1}$$

We call this map the modified Gumowski-Mira map, because [Gumowski and Mira, 1980a, Gumowski and Mira, 1980b] investigated the special case $a = 4/5$ and $b = 1$. For $b \neq -1$ this map has two fixed points. The origin is always a fixed point and it is attracting for $|a| < 1$. The other fixed point p is located at

$$p = \left(\frac{(1-a)}{(1+b)}, \frac{(1-a)}{(1+b)} \right).$$

For the special case considered in [Gumowski and Mira, 1980a, Gumowski and Mira, 1980b] the point p is a saddle with a negative stable eigenvalue. As is standard in such a situation, the stable set can be computed in this case by using the second iterate Q^2, but the folding Q^2 is more complex because its Jacobian is singular both when $DQ(x)$ or $D(Q(Q(x))$ are singular. By choosing different values for a and b this difficulty can be avoided. Specifically, we choose $a = -0.8$ throughout this paper and vary the parameter b; see also [England *et al.*, 2004]. Then the fixed point p is a saddle for $b < 3$, $b \neq -1$. The two

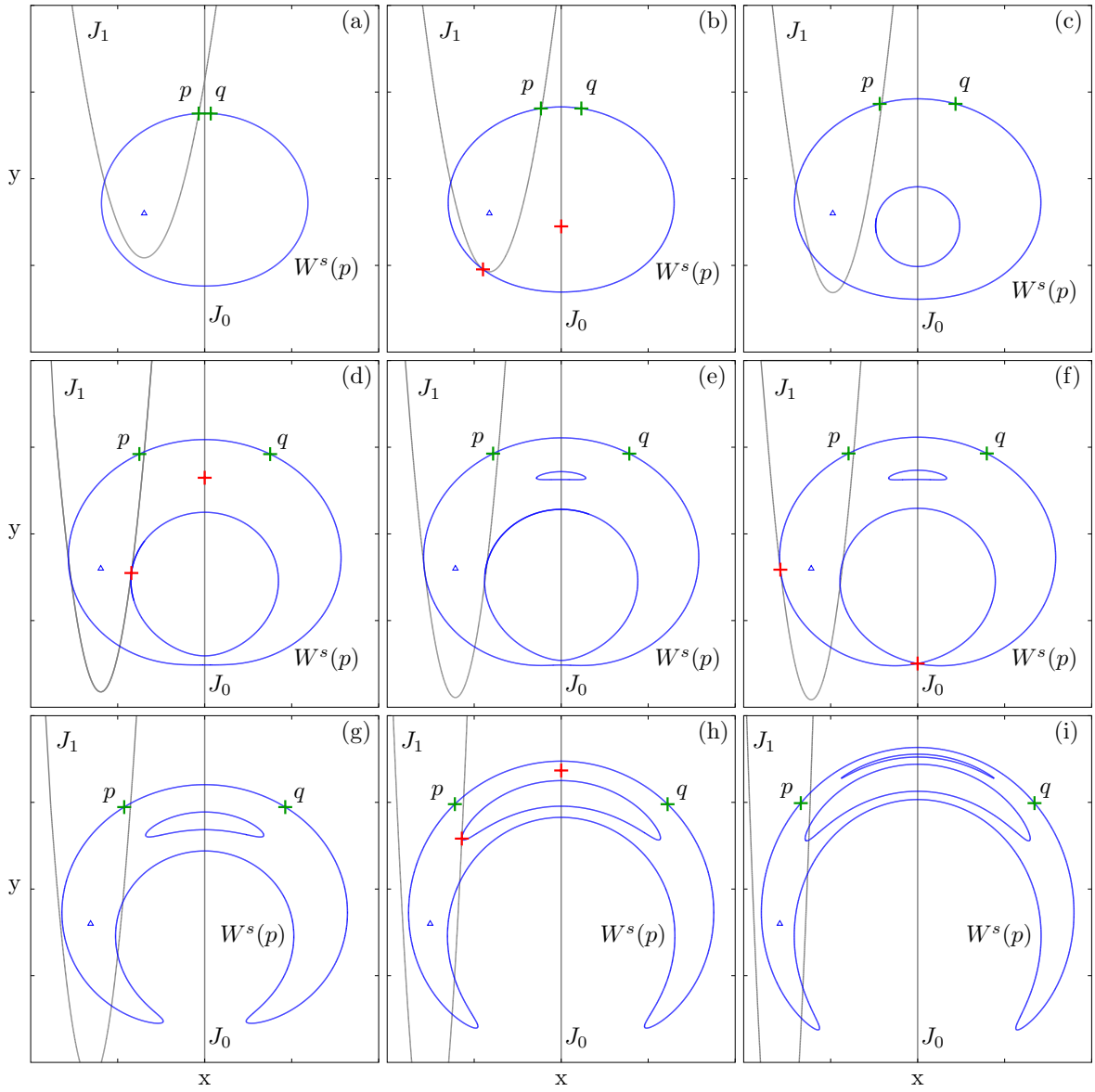

Figure 1: Bifurcations of the stable set $W^s(p)$ (blue curves) of the saddle p of (1) for $a = -0.8$ as b is varied. The curves J_0 and J_1 are shown in gray. The saddle point p and its pre-image q are indicated by green crosses. Tangency points between $W^s(p)$ and J_1 and their pre-images are indicated by red crosses. From (a) to (i) the parameter b takes the values 0.25, 0.18960, 0.14, 0.08995, 0.086, 0.0845735, 0.07, 0.04375, and 0.035.

sides of the primary manifold of the stable set of the saddle join to form a smooth closed loop. The area enclosed by the primary manifold is the basin of attraction of the sink.

The map (1) is designed such that the Jacobian matrix becomes singular along a vertical line, namely

$$J_0 := \left\{ x = -\frac{a}{2b} \right\}. \tag{2}$$

The rank-one critical curve is the parabola

$$J_1 := \left\{ y = x^2 - \frac{a^2}{4b} \right\}.$$

The phase plane folds along J_0 under Q, and the image of the fold J_1 divides the plane into two distinct regions, one with two pre-images and one with no pre-images, denoted Z_2 and Z_0, respectively. Since a fixed point always has at least one pre-image, namely itself, it must lie in Z_2. Hence, there is typically a distinct second pre-image of the saddle p, which we denote by q.

The map (1) has the reflectional symmetry of a perfect fold around J_0. This means that the points

$$\left(-\frac{a}{2b} \pm x,\, y \right)$$

map to the same point under Q. In particular, the point q is the mirror image of p and has the same y-coordinate, namely

$$q = \left(-\frac{(a+b)}{b(1+b)}, \frac{(1-a)}{(1+b)} \right).$$

2.1 Sequence of bifurcations of the stable set

In [England *et al.*, 2004] two particular cases $b = 0.2$ and $b = 0.1$ were used to illustrate the SC algorithm. Here we present a more detailed study of the bifurcation sequence as b is varied. Specifically, we can explain all bifurcations that we encounter by studying the interaction of the stable set with the critical curve J_1 in some small neighborhood.

Figure 1 shows the stable set for nine decreasing values of b. The scale of the vertical axes is the same in all panels, while the scale of the horizontal axes is adjusted, because the primary manifold is growing wider with decreasing $b > 0$. Specifically, the left point on the x-axis of each panel is fixed at $x = -3$ and the right point is chosen such that J_0 is always displayed at the center of each panel. The origin is a sink, and it is denoted by a blue triangle. In all panels the saddle p lies in the Z_2-region, above J_1, and its pre-image q lies in the Z_0-region, below J_1, as indicated by green crosses. The stable sets $W^s(p)$, including the primary manifold, are shown in blue and the critical curves J_0 and J_1 are shown in gray. The red crosses are either points where the stable set is tangent to J_1, or pre-images of these tangency points.

Figure 1(a) shows $W^s(p)$ for $b = 0.25$, where it only consists of the primary manifold that is connected to the saddle point. Both sides of the manifold join smoothly at q to

form a closed loop. All points on $W^s(p)$ map to the segment in the Z_2-region above J_1. The situation is topologically the same for $0.189860 < b < 3$. At $b \approx 0.189860$ the primary manifold $W^s(p)$ becomes tangent to J_1; see panel (b). We observe that the point of tangency has a double pre-image, which lies on J_0 (indicated by the red crosses). When decreasing b further, as is shown in panel (c) for $b = 0.14$, a new part of the stable set $W^s(p)$, namely a closed loop, is formed that is disconnected from the primary manifold. This so-called bubble has grown from the single point at the tangency and maps to the additional segment of the primary manifold that has moved above the J_1-curve. Panel (d) shows the case $b = 0.08995$, at which the disjoint bubble of the stable set is approximately tangent to J_1, giving rise to the birth of another disconnected closed curve, which will grow from the red cross; this is shown in panel (e) for $b = 0.086$. Approximately at $b = 0.0845735$, shown in Fig. 1(f), a tangency occurs at the left side of the picture, between the primary manifold and the curve J_1. We observe that the two separate segments of manifold that lie in the Z_2-region have joined. At the same time the original disjoint bubble of $W^s(p)$ connects with and then forms a part of the primary manifold. This connection happens at the pre-image of the tangency with J_1. Decreasing b further, the primary manifold now has the shape of a horseshoe; the situation for $b = 0.07$ is shown in panel (g) . The second bubble is still disconnected from the primary manifold. As this bubble grows with decreasing b, there is a tangency between this bubble and J_1 at approximately $b = 0.04375$; see panel (h). This bifurcation gives birth to a third disjoint bubble, which is shown in panel (i) for $b = 0.035$.

In the bifurcation sequence above, there are effectively only two different bifurcations that lead to the observed changes of the stable set $W^s(p)$. Both are generic codimension-one bifurcations where there is a tangency between $W^s(p)$ and J_1. The first bifurcation, which we call an *outer-fold bifurcation*, results in the creation (or disappearance) of a new isolated closed curve that belongs to $W^s(p)$. The second bifurcation, which we call an *inner-fold bifurcation*, changes the local connectedness of branches of $W^s(p)$. Each of these bifurcations is discussed in detail from the point of view of bifurcation theory in the next section.

We finish this section by showing what happens if b is decreased further towards zero. Since the formula (2) for J_0 has b in the denominator, the curve J_0 tends to infinity in the limit as b approaches zero. For $b = 0$ the map (1) is actually a diffeomorphism, that is, each point has a unique pre-image and the map Q is invertible. In particular, the saddle p still exists, but its second pre-image q does not. Furthermore, $W^s(p)$ must be a simply connected smooth stable manifold. Hence, as b gets closer to zero all bubbles must disappear. Figure 2 gives an indication of how this happens with the three phase portraits for $b = 0.014$ (a), $b = 0.01306669$ (b), and $b = 0.0125$ (c). The bubbles are joined one by one to the primary manifold in inner-fold bifurcations; compare Fig. 2(b). As b tends to zero the left branch of $W^s(p)$ retracts further and further into the Z_2-region and, since J_0 disappears to infinity, the right branch goes off to infinity for $b = 0$.

3 Generic codimension-one bifurcations of stable sets

The outer-fold and inner-fold bifurcations in Sec. 2 underlie various types of 'basin bifurcations' [Cathala, 1998, Kitajima *et al.*, 2000, Mira *et al.*, 1994] and 'contact bifurcations'

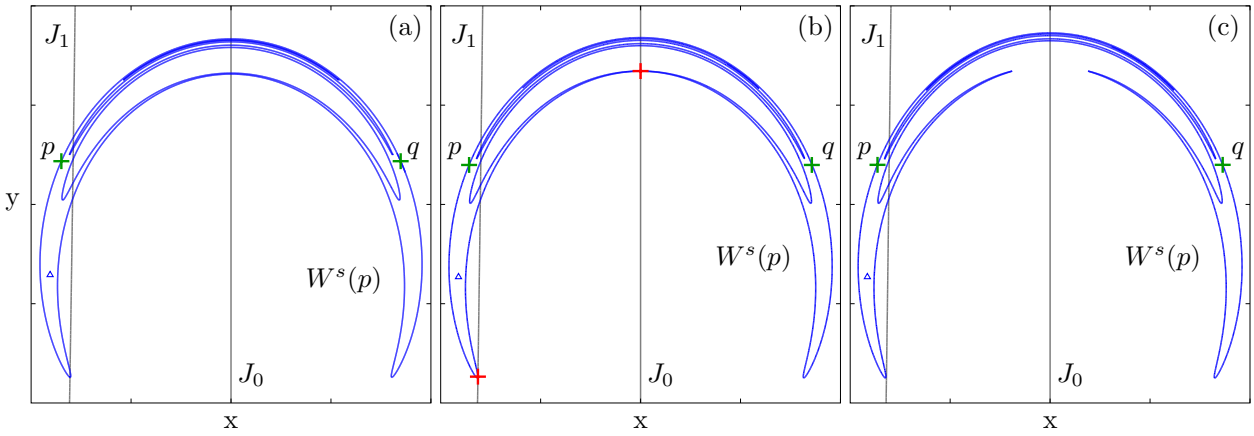

Figure 2: Further bifurcations of the stable set $W^s(p)$ of the saddle p of (1) for $a = -0.8$; compare Fig. 1. From (a) to (c) the parameter b takes the values 0.014, 0.01306669, and 0.0125, while the curve J_0 is at $x = 28.571$, $x = 30.612$ and $x = 32$, respectively. As $b \to \infty$ the disjoint bubbles disappear in inner-fold bifurcations; one such inner-fold bifurcation is shown in panel (b).

[Agliari, 2000, Agliari *et al.*, 2003, López-Ruiz and Fournier-Prunaret, 2003] that can be found in the literature. As was mentioned in the introduction, these bifurcations were not viewed in the first instance as bifurcations of a stable set, but as bifurcations of a basin of attraction. Because the underlying outer-fold or inner-fold bifurcations can change a given basin of attraction in different ways, they are associated with many different names, depending on their 'global flavor' and which basin of attraction is under consideration. Indeed the notation in the literature is rather complicated. It is generally related to the connectedness of the basin of attraction and some papers even contain a glossary of the names that are given to the different bifurcations [López-Ruiz and Fournier-Prunaret, 2003, Mira *et al.*, 1994].

The main point of this paper is to take the point of view of bifurcation theory and singularity theory, in order to provide a systematic way of classifying qualitative changes to the stable set and, hence, to basins of attraction. To this end, we first consider the *generic codimension-one bifurcations* where the stable set interacts with the critical curve J_1. The assumption that the codimension-one bifurcation be generic means, in particular, that the stable set crosses the critical curve J_1 at a generic point, that is, at an image of a regular fold point of J_0. Furthermore, genericity demands that the stable set and J_1 have a quadratic tangency. (We do not consider here the case that the stable set and J_1 already have a generic crossing, in which case the generic bifurcation would be a cubic tangency.) In other words, there are exactly two *generic codimension-one bifurcations* where the stable set crosses J_1 upon change of a parameter, namely the outer-fold and inner-fold bifurcations we already encountered in the previous section. We stress that this is true irrespective of the particular folding structure of the given map.

These two bifurcations, when seen only in a local neighborhood of the tangency, are the basic building blocks of any change in the structure of a basin boundary when a single parameter is varied. The second step is to consider the *global arrangement of the stable set*

at the moment that it undergoes either an outer-fold or an inner-fold bifurcation. Since there are different possibilities of connecting branches of the stable set globally, there are different ways in which a outer-fold or inner-fold bifurcation manifests itself, for example, when one is interested in the change of a basin of attraction. In this way, all changes to a given basin of attraction, including changes to its local connectedness, can be understood and classified in a systematic way as a combination of an outer-fold or inner-fold bifurcation with a particular 'global flavor'.

3.1 Outer-fold bifurcation

The outer-fold bifurcation occurs when a segment of the stable set becomes tangent to the J_1 curve on the outer side of the fold, so that a segment of the stable set crosses into the region with two extra pre-images. The additional pre-images of this segment form a disjoint bubble that is part of the stable set.

Figure 3 demonstrates how the outer-fold bifurcation creates a disjoint bubble by using data for the map (1). The illustration is in the spirit of singularity theory and shows the folded phase plane in such a way that the action of the map f can be interpreted as a simple projection onto regions near J_0 and J_1, respectively. Indeed, a local neighborhood of J_0, shown as a vertical plane, maps to a local neighborhood of J_1, shown as a horizontal plane. It is indicated in the figure that the stable set crosses from a region Z_k with k pre-images into a region Z_{k+2} with $k+2$ pre-images. However, because we only consider the situation locally near the tangency point, this is (locally) equivalent to the case of a Z_0–Z_2 map, such as (1).

For $b = 0.25$ a segment of the stable set is shown in light blue. Since it does not intersect J_1 it has k pre-images (outside the local neighborhood that we are interested in). For $b = 0.189860$ the stable set is shown in a darker blue and it is tangent to J_1. This means that the intersection point on $W^s(p)$ and J_1 (red cross) has one extra (double) pre-image, which is illustrated by projecting the point up to the folded plane and then across, giving the double pre-image (also denoted by a red cross) on the curve J_0. The stable set for $b = 0.14$ is shown in even darker blue and it crosses J_1 into the folded region, so that a whole segment of the manifold lies in the Z_{k+2}-region. If one projects this piece of manifold up to the folded plane and then across to the unfolded phase plane, it is clear how the disjoint bubble is formed around the pre-image of the tangency point on J_0. Note that the piece of the stable set in the Z_{k+2}-region has k other pre-images, which do not take part in the bifurcation; they correspond to the k pre-images in the Z_k-region.

We remark that an outer-fold bifurcation occurs three times in the bifurcation sequence shown in Fig. 1, namely in panels (b), (d) and (h). Each case is different with respect to which part of the stable set has an outer-fold bifurcation with J_1. For example, in panel (d) there is a tangency of the first bubble with the curve J_1, leading to the creation of the second bubble. As is shown in Fig. 4, this bifurcation can be interpreted as a tangency of the primary manifold with the curve $J_2 = f(J_1)$. Indeed, all images of tangencies are again tangencies of the respective images.

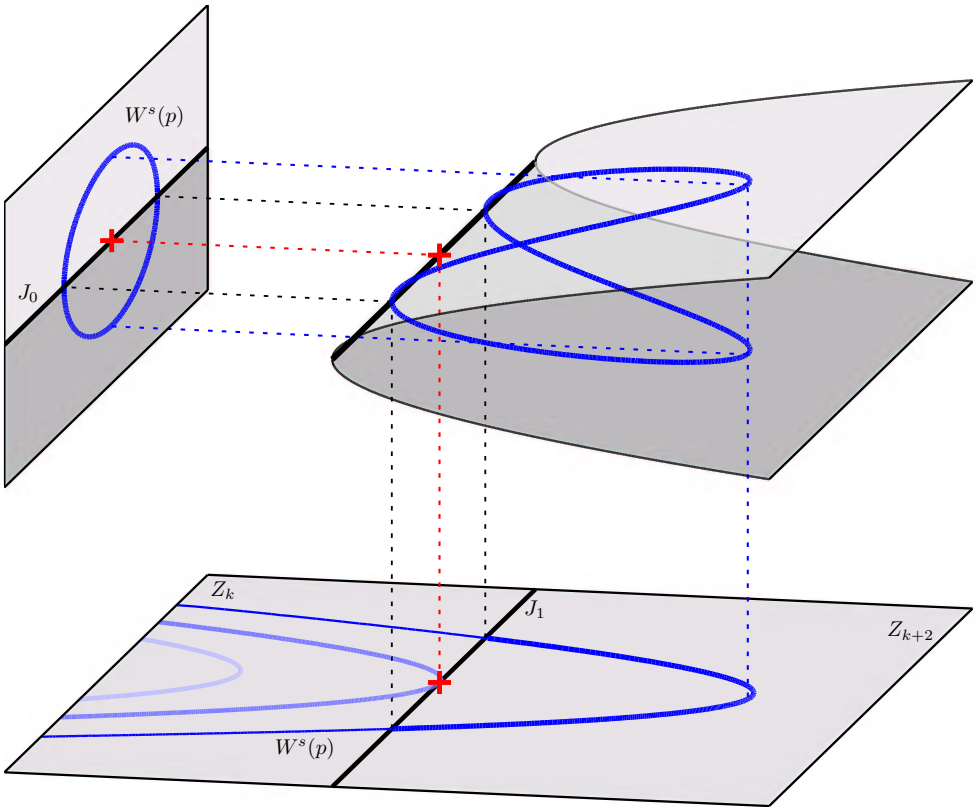

Figure 3: A schematic representation of the outer-fold bifurcation. The map f folds the vertical plane along J_0 and maps it to the right of J_1 onto the horizontal plane. There are two regions Z_k and Z_{k+2} to the left and right of J_1 with k and $k+2$ rank-one pre-images, respectively. The stable set $W^s(p)$ does not intersect J_1 before the bifurcation, but is tangent to J_1 at the outer-fold bifurcation, and has two intersection points with J_1 after the bifurcation. After the bifurcation a part of $W^s(p)$ extends into the region Z_{k+2} where there are (locally) two extra pre-images. This part of $W^s(p)$ lifts to the folded phase plane, resulting in an isolated closed curve near the pre-image of the tangency point on J_0. The shown manifolds are (scaled) data of the map (1) for $a = -0.8$ and $b = 0.25$, $b = 0.189860$ and $b = 0.14$, respectively.

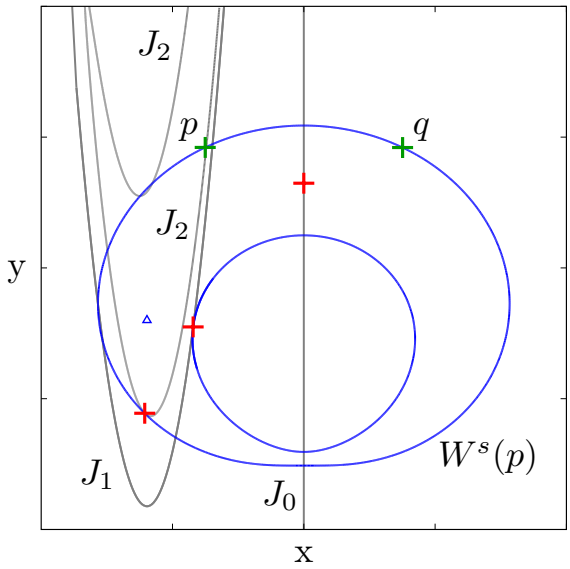

Figure 4: The stable set $W^s(p)$ (blue curves) of (1) for $a = -0.8$ and $b = 0.08995$ shown together with the curves J_0, J_1 and $J_2 = f(J_1)$ (gray curves). The saddle point p and its pre-image q are indicated by green crosses. A tangency between the disjoint bubble and J_1 must map to a tangency between the primary manifold and J_2. The pre-image on J_0 of the tangency with J_1 is then the onset of a new disjoint bubble. Tangencies and their pre-images are indicated by red crosses.

3.2 Inner-fold bifurcation

The inner-fold bifurcation occurs when a segment of the stable set becomes tangent to the curve J_1 on the inner side of the fold, so that a segment of the stable set crosses into the region with two less pre-images. This leads to a different connectivity between the four branches of the stable set that are involved in this bifurcation. Figure 5 demonstrates this with data for the map (1). The three panels (a)–(c) show the situation before, at and after the inner-fold bifurcation in the same way as Fig. 3. Again, a local neighborhood of J_0, shown as the vertical plane, maps to a local neighborhood of J_1, shown as the horizontal plane.

Before the tangency, in Fig. 5(a), the stable set locally extends across J_1 into the Z_k-region. The two segments in the Z_{k+2}-region each have two (local) pre-images which are connected across J_0 as indicated by the vertical plane, the projection to a local neighborhood of J_0. At the inner-fold bifurcation the stable set is tangent to J_1 and the two segments in the Z_{k+2}-region connect at the tangency point with J_1, indicated again by the red cross. Therefore, their pre-images are also connected at a single point on J_0. After the bifurcation the stable set remains entirely inside the Z_{k+2}-region. Its two disjoint pre-images do not connect across J_0 any longer, which means that the connectivity of the branches near J_0 has changed. As before, the k other pre-images of the stable set do not take part in the bifurcation.

We remark that an inner-fold bifurcation occurs in Fig. 1(f). The change of the local

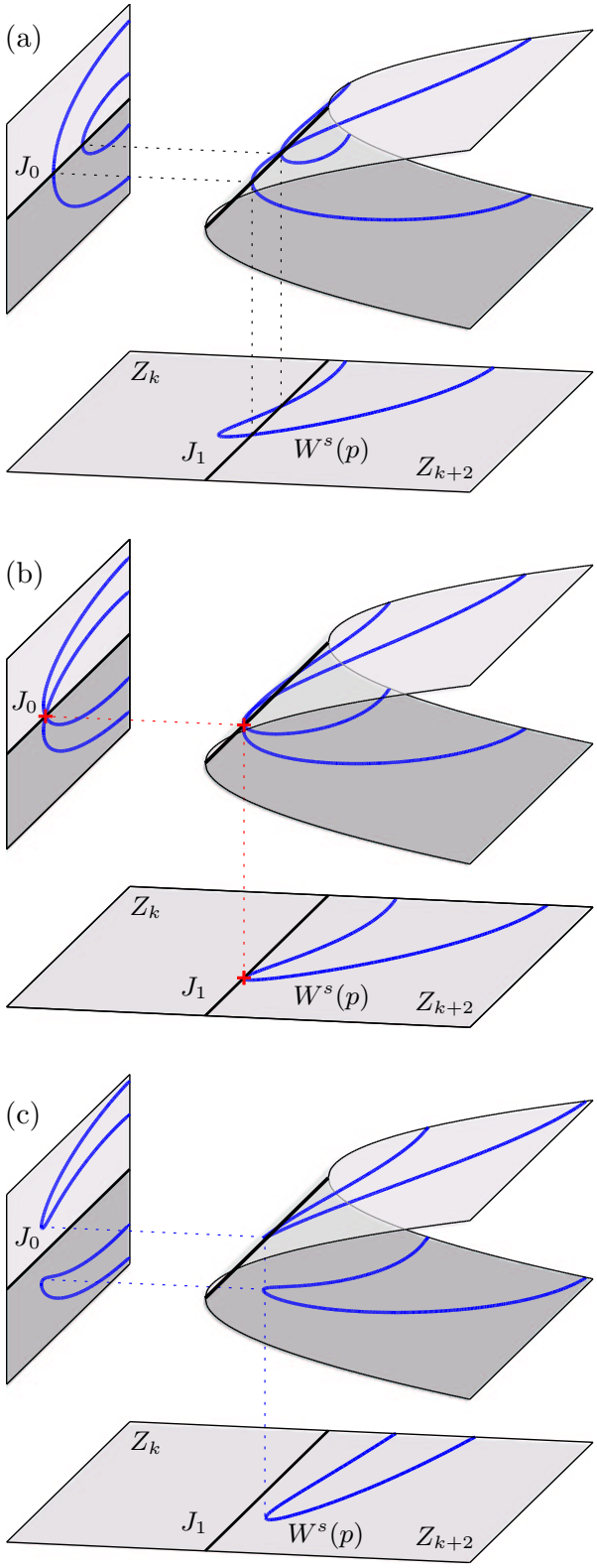

Figure 5: A schematic representation of the inner-fold bifurcation, illustrated in the same way as in Fig. 3. The three panels show the local phase portraits before (a), at (b), and after (c) the inner-fold bifurcation using (scaled) data from (1) for $a = -0.8$ and $b = 0.086$, $b = 0.0845735$ and $b = 0.07$, respectively.

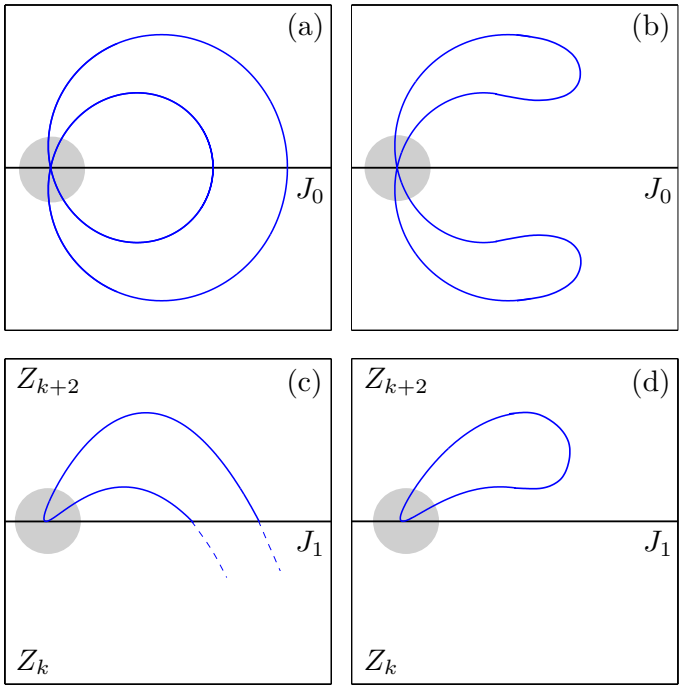

Figure 6: Two different global flavors of the inner-fold bifurcation. The stable sets in panels (a) and (b) are mapped to the Z_{k+2}-region as shown in panels (c) and (d), respectively. Panels (a) and (c) demonstrate the case where, at the bifurcation, the stable set intersects J_1 outside a local neighborhood of the tangency point, while in (b) and (d) the stable set does not intersect J_1 outside a local neighborhood.

connectivity can clearly be seen by comparing panels (e) and (g). Since the branches of the stable set involve the primary manifold and the first bubble, this inner-fold bifurcation manifests itself as a qualitative change of the primary manifold.

3.3 Different global flavors of the inner-fold bifurcation

The overall or global manifestation of an inner-fold bifurcation depends on which part of the stable set crosses J_1. Furthermore, it is important to know how the pre-images of the two segments of the stable set, which meet at the pre-image of the tangency point, are connected *outside the local neighborhood* that we consider.

Figure 6 shows two topologically different global phase portraits at the moment of an inner-fold bifurcation. Both agree in the small gray neighborhood, but the global structure outside this gray neighborhood is different. In panel (a) the two branches are connected across J_0 outside a neighborhood of the point where they meet. We have already seen this possibility for the inner-fold bifurcation in Fig. 1(e)–(g). This means that the stable set must cross J_1 at two different points, as shown in the image under f in panel (c). In Fig. 6(b), on the other hand, the two branches are connected in such a way that they do not cross J_0 outside a neighborhood of the point where they meet. This means that the image, shown

in panel (d), remains entirely inside the Z_{k+2}-region. In this case, the stable set in panel (b) takes the form of a pinched bubble. In the unfolding of the inner-fold bifurcation a single bubble that crosses J_0 at two nearby points pinches and then splits into two separate bubbles.

4 Bifurcations of basin boundaries

The bifurcations of the stable set that we discussed so far can be interpreted directly as bifurcations of basins of attraction. To make this point, we show in Fig. 7 four instances of panels from Fig. 1 where we colored the basin of the origin in green and the basin of infinity in blue. The coloring is motivated by the literature on basins of attraction that speaks of 'sea', 'land', 'lakes' and 'islands'. Indeed, as noted in [Kitajima *et al.*, 2000, Mira *et al.*, 1994], 'islands' and 'lakes' are equivalent, simply by exchanging the coloring of the respective basins.

Figure 7(a) shows a situation where the basin of attraction is a simply connected domain. However, as is clear from the other panels in Figure 7, a basin of attraction of a noninvertible map need not be simply connected. While the literature speaks of the changes to the 'island number' or 'lake number' [Mira *et al.*, 1994], a topological classification of a basin of attraction would require one to consider its fundamental group and how it changes in bifurcations.

In this paper we argue that the notation in the literature is rather phenomenological, leading to many seemingly different cases, while the underlying bifurcation is always either an outer-fold or an inner-fold bifurcation of a particular global flavor. For example, an outer-fold bifurcation leads to the situation in Figure 7(b) where the green basin is multiply connected (has a nontrivial fundamental group). In the literature one often finds the description that the green basin, which is an 'island' or 'continent' in the 'sea', has a 'hole' or 'lake'. The bifurcation itself has been called a 'connected basin $\leftrightarrow$ multiply connected basin bifurcation' when seen from the point of view of the green basin of the origin; it has also been called a 'connected basin $\leftrightarrow$ disconnected basin bifurcation', when seen from the point of view of the blue basin of infinity [Mira *et al.*, 1994]. (These two names are equivalent in the case of only two basins, because the green basin being simply connected means by definition that the blue basin is connected, and vice versa.) The second outer-fold bifurcation changes the connectivity of the green basin again. As shown in Figure 7(c), there are now two 'lakes' (and the fundamental group has two generators). As far as we are aware, any further increase in the connectivity of a basin is referred to in the literature as a change to either the 'island number' or the 'lake number' [Mira *et al.*, 1994].

Finally, in an inner-fold bifurcation with the global flavor as was shown in Fig. 6(a) and (c), the connectivity of the green basin changes again. As is shown in Fig. 7(d), the 'lake' has now joined the 'sea', which is also referred to as a 'lake $\leftrightarrow$ roadstead' bifurcation [Mira *et al.*, 1994]. The fundamental group becomes smaller, and the topology of the basins in Fig. 7(d) is just like that in Fig. 7(b).

In summary, changes to the connectivity of a basin of attraction can be classified in the spirit of bifurcation theory by only two ingredients: whether an outer-fold or an inner-fold bifurcation is involved and the global organization of the stable set at the moment of

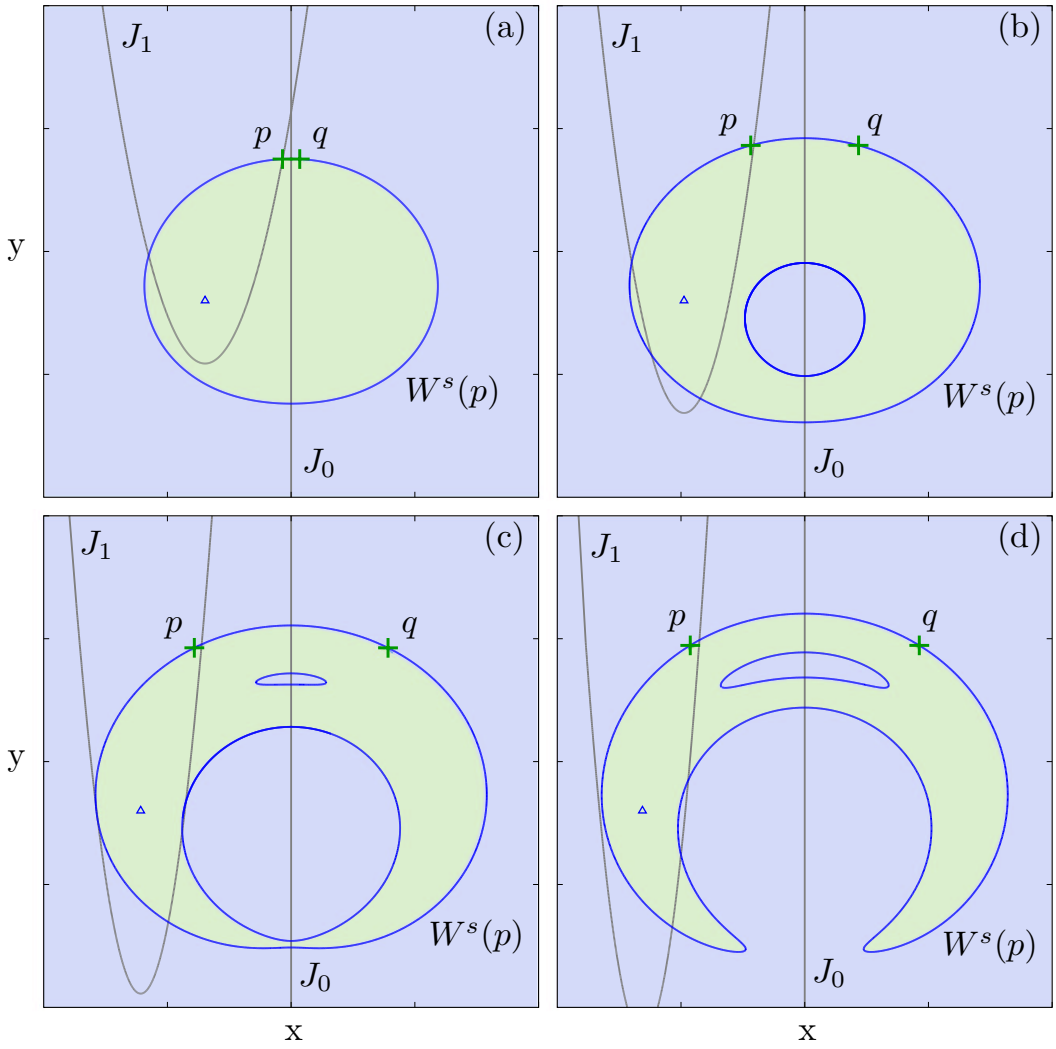

Figure 7: The stable sets of (1) for $b = 0.25$ (a), $b = 0.14$ (b), $b = 0.086$ (c), and $b = 0.07$ (d). The green shaded area indicates the basin of attraction for the origin (blue triangle). The blue shaded area indicates the basin of attraction of infinity.

bifurcation. The latter involves information about which part of the stable set, the primary branch or a disjoint piece, undergoes the bifurcation and how branches are connected outside a neighborhood of the bifurcation point.

5 Stable set versus unstable manifold

If one considers an invertible map, that is, a diffeomorphism, then the stable manifold is the unstable manifold of the inverse f^{-1}, and vice versa. However, for a noninvertible map f as considered here this duality between stable and unstable manifolds does not exist. Indeed, there is a fundamental difference between the stable set $W^s(\mathbf{x}_0)$ of a saddle point $\mathbf{x}_0$ and the unstable manifold $W^u(\mathbf{x}_0)$. This means that one also finds fundamentally different

bifurcations when these sets interact with the curves J_0 and J_1.

By definition, the *global unstable manifold* $W^u(\mathbf{x}_0)$ consists of points that converge to $\mathbf{x}_0$ under backward iteration, that is, under application of any sequence of inverse branches of f. In terms of forward iterates this can be expressed as

$$W^u(\mathbf{x}_0) = \left\{ x \in \mathbb{R}^2 \;\middle|\; \exists \{q_k\}_{k=0}^{\infty},\, q_0 = x \text{ and } f(q_{k+1}) = q_k, \text{ such that } \lim_{k\to\infty} q_k = \mathbf{x}_0 \right\}.$$

Because we assume that the Jacobian is nonsingular at $\mathbf{x}_0$, there exists the local unstable manifold $W^u_{loc}(\mathbf{x}_0)$, which is associated with the unique inverse branch that fixes $\mathbf{x}_0$. The global unstable manifold $W^u(\mathbf{x}_0)$ can then be expressed as

$$W^u(\mathbf{x}_0) = \bigcup_{n=1}^{\infty} f^n(W^u_{loc}(\mathbf{x}_0)). \tag{3}$$

Note that even for noninvertible f the images of $W^u_{loc}(\mathbf{x}_0)$ are unique. Indeed there may be other pre-images of $W^u(\mathbf{x}_0)$, but these are not part of $W^u(\mathbf{x}_0)$ because points in these pre-images do not converge to $\mathbf{x}_0$ under backward iteration. Overall, $W^u(\mathbf{x}_0)$ is an immersed manifold in the phase space (it may have self-intersections as is discussed below), so that it is justified to speak of $W^u(\mathbf{x}_0)$ as the *unstable manifold*. Furthermore, the unstable manifold $W^u(\mathbf{x}_0)$ can be computed numerically with any algorithm that was developed for invertible maps.

As we have seen, an interaction between the stable set $W^s(\mathbf{x}_0)$ and the critical curve J_1 leads to a bifurcation occurring in the neighborhood of its pre-images on J_0. For the unstable manifold $W^u(\mathbf{x}_0)$, the converse is true: one needs to consider the interaction between $W^u(\mathbf{x}_0)$ and the curve J_0 where the Jacobian is singular.

A transverse intersection of $W^u(\mathbf{x}_0)$ with J_0 generically corresponds in the image to a tangency between $W^u(\mathbf{x}_0)$ and J_1. The genericity condition is that the tangent to $W^u(\mathbf{x}_0)$ at the crossing point with J_0 (which is, in fact, the eigenvector of the zero eigenvalue) does not coincide with the normal to J_0 at this point. A codimension-one bifurcation occurs when this genericity condition is violated. This is sketched in Fig. 8, where panels (a) and (c) show structurally stable tangencies of $W^u(\mathbf{x}_0)$ with J_1. At the bifurcation point, sketched in Fig. 8 (b), the tangent to $W^u(\mathbf{x}_0)$ and the normal to J_0 at the crossing point coincide. This means that $W^u(\mathbf{x}_0)$ has a cusp point where $W^u(\mathbf{x}_0)$ and J_1 meet. This bifurcation leads to the creation of a structurally stable, transverse self-intersection and a little loop of $W^u(\mathbf{x}_0)$ in a neighborhood of the image near J_1, as shown in Fig. 8(c). Note that there is a clear sense of direction along $W^u(\mathbf{x}_0)$ even when it has loops. Since $W^u(\mathbf{x}_0)$ is invariant under f, this bifurcation creates infinitely many self-intersections and loops, which are the images under f^l (for any integer $l \geq 1$) of the intersection point of $W^u(\mathbf{x}_0)$ with J_0.

Self-intersections and the associated loops of an unstable manifold have been reported in the literature; see [Lorenz, 1989], where the loops are called 'antennae', and [Frouzakis *et al.*, 1997, Frouzakis *et al.*, 2003, Maistrenko *et al.*, 2003, Mira *et al.*, 1996b]. These authors are mainly interested in bifurcations leading to the destruction of an invariant curve (also called 'IC' or 'torus'), which is the closure of unstable manifolds of suitable periodic points. The development of cusps and then loops of the unstable manifold is interpreted as a global bifurcation of the invariant curve. For example, [Frouzakis *et al.*, 2003, p. 107] report the 'destruction of the IC through a global bifurcation, appearance of loops on an unstable manifold,

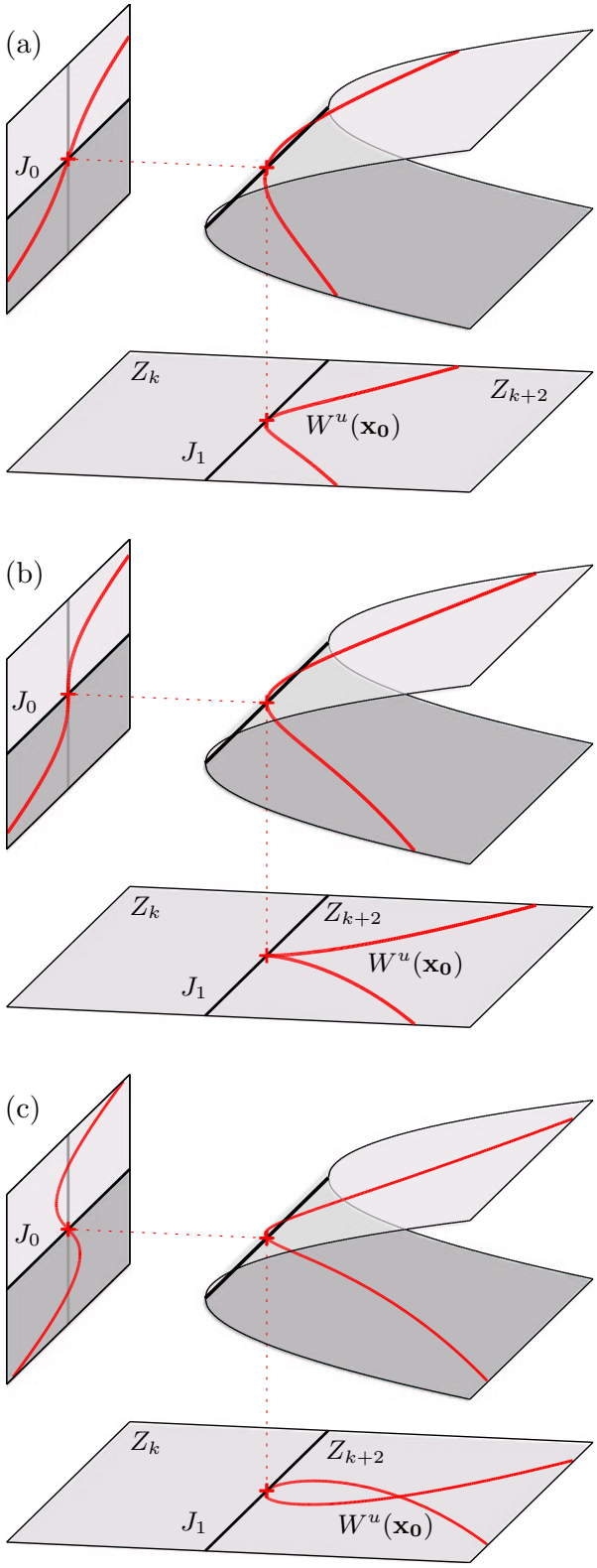

Figure 8: The loop bifurcation, illustrated as in Fig. 3. The three panels show the unstable manifold (red curve) in a local neighborhood before (a), at (b), and after (c) the bifurcation; the gray line in the vertical phase plane is the direction normal to J_0 at the crossing point with $W^u(\mathbf{x}_0)$. The panels were obtained from the normal form (4) for $\mu = 1$, $\mu = 0$ and $\mu = -1$, respectively.

and the reappearance of an attractor, this time chaotic with loops'. The ensuing global attractor 'inherits' loops from the global unstable manifold, and this type of attractor has been called a 'weakly chaotic ring' [Frouzakis *et al.*, 1997, Mira *et al.*, 1996b]. The papers [Frouzakis *et al.*, 1997], [Frouzakis *et al.*, 2003] and [Maistrenko *et al.*, 2003] contain explanations of how loops are formed. In [Frouzakis *et al.*, 1997, p. 1178] the point on J_1 around which the loop forms is called a 'self intersection of projection'. Both [Frouzakis *et al.*, 2003] and [Maistrenko *et al.*, 2003] state the condition that the eigenvector corresponding to the zero eigenvalue coincides with the normal to J_0 at the moment when the unstable manifold develops cusps. However, none of these authors gives this codimension-one bifurcation a name or describes it in the spirit of bifurcation theory.

It does not appear to have been reported explicitly in the literature that this codimension-one bifurcation is given by a cubic tangency of $W^u(\mathbf{x}_0)$ with respect to the normal vector of J_0, and that it simply unfolds as a cusp singularity. This can be seen in the vertical neighborhood, on the left in Fig. 8, around the transverse crossing point of $W^u(\mathbf{x}_0)$ and J_0. The unfolding can be written as the normal form

$$R(s) = \mu s - s^3 \tag{4}$$

in the (r, s)-plane, where $J_0 = \{s = 0\}$, the normal vector is $(0, 1)$, $W^u(\mathbf{x}_0) = \text{graph}(R)$ and μ is the unfolding parameter. Figure 8 was obtained by using the normal form (4) in the vertical neighborhood near J_0 and then using projections via the folded plane to the horizontal neighborhood of J_1. To avoid confusion with the codimension-two cusp bifurcation of equilibria, we call this codimension-one bifurcation of the unstable manifold the *loop bifurcation.*

We finish this section with a contrasting statement.

Proposition 1. *The stable set $W^s(\mathbf{x}_0)$ of a hyperbolic saddle point $\mathbf{x}_0$ of a noninvertible map $f : \mathbb{R}^n \to \mathbb{R}^n$, $n > 1$, cannot have structurally stable self-intersections.*

Proof. Since $\mathbf{x}_0$ is hyperbolic it does not lie on J_0, so that there is a small neighborhood U of $\mathbf{x}_0$ in which f is a local diffeomorphism (taking again the appropriate branch of the inverse). Hence, $W^s_{\text{loc}}(\mathbf{x}_0) \in U$ does not have self-intersections.

Consider now a transverse intersection of two branches of $W^s(\mathbf{x}_0)$ in some neighborhood V. Since the intersection point $t \in V$ is on the stable set, it must map under some iterate of f, say, under f^L, onto $W^s_{\text{loc}}(\mathbf{x}_0) \in U$.

Suppose now that the intersection point t does not lie on the set of preimages $\cup_{0 \le l \le L} f^{-l}(J_0)$ of J_0. Then all iterates f^l for $1 \le l \le L$ are diffeomorphisms on the neighborhood V. In particular, $f^L(V)$ contains a transverse intersection of two branches of $W^s(\mathbf{x}_0)$. Since $f^L(t) \in f^L(V) \cap U \neq \emptyset$ we have found a transverse intersection in U, which is a contradiction.

In other words, we must have that $f^l(t) \in J_0$ for some $0 \le l \le L$. This shows that the self-intersection t of $W^s(\mathbf{x}_0)$ is not structurally stable, because a small perturbation of f destroys this property. □

The condition that $f^l(t) \in J_0$ means that, generically, we find a codimension-one inner-fold bifurcation at $f^l(t)$ as was described in Sec. 3.2. In other words, the last self-intersection unfolds as shown in Fig. 5.

Note that Proposition 1 was formulated for a saddle point $\mathbf{x}_0$ for convenience and can be generalised to stable sets of other hyperbolic invariant set of saddle type. In particular, the statement holds for a saddle periodic orbit simply by means of considering an appropriate iterate of f.

6 Conclusions

Bifurcations of stable sets in noninvertible planar maps occur when the stable set interacts with a critical curve where the number of pre-images changes. It is now possible to compute stable sets and find such bifurcations directly. Note that a method for computing the regions of different numbers of pre-images of noninvertible maps has been developed [Nien and Wicklin, 1998] and implemented in the program PISCES [Wicklin, 1995].

We considered a generic codimension-one bifurcation of the stable set, of which there are exactly two cases, the outer-fold and the inner-fold bifurcation. Both were illustrated with data from an example family of noninvertible maps. Furthermore, we contrasted the properties of the stable set with that of the unstable manifold. We showed how the unstable manifold may develop structurally stable self-intersections, while this is not possible for the stable set.

It must be stressed that the results presented here are valid for any noninvertible map, irrespective of its particular folding of the phase plane. This is so because the generic case is always a quadratic tangency with a critical curve along which the number of pre-images changes by two. Furthermore, the outer-fold and the inner-fold bifurcation are the generic codimension-one interactions of any invariant curve (not necessarily a segment of a stable set) with the critical curve. In other words, the unfoldings presented here are equally valid, for example, to describe bifurcations of invariant circles.

Since a basin boundary of a noninvertible planar map is typically bounded by stable sets, the two outer-fold and the inner-fold bifurcations lead to changes in the structure of a given basin. In fact, we argued that all changes to basins of attraction can be classified in the spirit of bifurcation theory by the type of bifurcation in combination with its 'global flavor', by which is meant the global structure of the part of the stable set that undergoes the bifurcation.

Obvious future work is the consideration of generic bifurcations of stable sets (or invariant curves) of higher codimension. The codimension may be increased by interacting with the critical curve at non-generic points, for example a cusp. Alternatively, one may look at a non-quadratic (quartic) tangency with a generic segment of the critical curve.

Finally, we mention that the general approach presented here may be used to consider noninvertible maps on higher-dimensional spaces. The next step would be to consider noninvertible maps of $\mathbb{R}^3$. This is already quite a challenge. One now deals with a two-dimensional critical manifold J_1 (instead of a critical curve) along which the number of pre-images changes. Clearly, the singularity theory of smooth noninvertible maps of $\mathbb{R}^3$ is more complicated than that of smooth noninvertible maps of $\mathbb{R}^2$. Furthermore, the stable set may be up to two-dimensional.

7 Acknowlegdements

We thank Yuri Maistrenko and Bruce Peckham for helpful discussions. The research of J.E. was supported by grant GR/R94572/01 from the Engineering and Physical Sciences Research Council (EPSRC).

References

Abraham, R. H., Gardini, L. and Mira, C. [1997] *Chaos in discrete dynamical systems: a visual introduction in 2 dimensions*, Springer-Verlag, New York.

Arnol′d, V. I. [1992] *Catastrophy Theory*, third revised and expanded edition, Springer-Verlag, Berlin.

Adomaitis, R. A. and Kevrekidis, I. G. [1991] "Noninvertibility and structure of basins of attraction in a model adaptive control system," *J. Nonlin. Sci.* **1**, 95–105.

Agliari, A. [2000] "Global bifurcations in the basins of attraction in noninvertible maps and economic applications," *Proceedings of the Third World Congress of Nonlinear Analysts, Part 8* [2001] (Catania, 2000). *Nonlinear Anal.* **47**(8), 5241–5252.

Agliari, A., Gardini, L. and Mira, C. [2003] "On the fractal structure of basin boundaries in two-dimensional noninvertible maps," *Int. J. Bifurcation and Chaos* **13**(7), 1767–1785.

Back, A., Guckenheimer, J., Myers, M. R., Wicklin, F. J. and Worfolk, P. A. [1992] "DsTool: Computer assisted exploration of dynamical systems," *Notices Amer. Math. Soc.* **39**, 303–309.

Cathala, J. C. [1998] "Basin properties in two-dimensional noninvertible maps," *Int. J. Bifurcation and Chaos* **8**(11), 2147–2189.

England, J. P., Krauskopf, B. and Osinga, H. M. [2004] "Computing one-dimensional stable manifolds and stable sets of planar maps without the inverse," *SIAM J. on Applied Dynamical Systems*, **3**(2), 161–190.

Frouzakis, C. E., Adomaitis, R. A., Kevrekidis, I. G., Golden, M. P. and Ydstie, B. E. [1992] "The structure of basin boundaries in a simple adaptive control system" *Proc. NATO 1992, Advanced Summer Institute* (Ed. Bountis T.), pp. 195–210.

Frouzakis, C. E., Adomaitis R. A. and Kevrekidis, I. G. [1996] "An experimental and computational study of subcriticality, hysteresis and global dynamics for a model adaptive control system," *Computers Chem. Engng* **120**, 1029–1034.

Frouzakis, C. E., Gardini, L., Kevrekidis, I. G., Millerioux, G., and Mira, C. [1997] "On some properties of of invariant sets of two-dimensional noninvertible maps," *Int. J. Bifurcation and Chaos* **7**(6), 1167–1194.

Frouzakis, C. E., Kevrekidis, I. G. and Peckham, B. [2003] "A route to computational chaos revisited: noninvertibility and the breakup of an invariant circle," *Physica D* **177**, 101–121.

Gumowski, I. and Mira, C. [1977] "Solutions chaotiques bornée d'une récurrence ou transformation ponctuelle du second ordre à inverse non-unique," *Comptes Rendus Acad. Sc. Paris* **A285**, 477–480.

Gumowski, I. and Mira, C. [1980a] *Dynamique Chaotique*, Ed. Cepadues, Toulouse.

Gumowski, I. and Mira, C. [1980b] *Recurrences and Discrete Dynamic Systems*, Springer-Verlag, New York.

Kitajima, H., Kawakami, H. and Mira, C. [2000] "A method to calculate basin bifurcation sets for a two-dimensional noninvertible map," *Int. J. Bifurcation and Chaos* **10**(8), 2001–2014.

López-Ruiz, R. and Fournier-Prunaret, D. [2003] "Complex patterns on the plane: different types of basin fractalization in a two-dimensional mapping," *Int. J. Bifurcation and Chaos* **13**(2), 287–310.

Lorenz, E. N. [1989] "Computational chaos - a prelude to computational instability," *Physica D* **35**, 299–317.

Maistrenko, V., Maistrenko, Y. and Sushko, I. [1996] "Noninvertible two-dimensional maps arising in radiophysics," *Int. J. Bifurcation and Chaos*, **4**(2), 383–400.

Maistrenko, V., Maistrenko, Y. and Mosekilde, E. [2003] "Torus breakdown in noninvertible maps" *Phys. Rev. E* **67**, 046215.

Mira, C., Fournier-Prunaret, D., Gardini, L., Kawakami, H. and Cathala, J. C. [1994] "Basin bifurcations of two-dimensional noninvertible maps: fractalization of basins," *Int. J. Bifurcation and Chaos* **4**(2), 343–381.

Mira, C., Jean-Pierre, C., Millérioux, G. and Gardini, L. [1996a] "Plane foliation of two-dimensional noninvertible maps," *Int. J. Bifurcation and Chaos* **6**(8), 1439–1462.

Mira, C., Gardini, L., Barugola, A. and Cathala, J. C. [1996b] *Chaotic dynamics in two-dimensional noninvertible maps*, Nonlin. Sci. Series A, World Scientific, Singapore.

Rico-Martinez, R., Adomaitis, R. A. and Kevrekidis, I. G. [2000] "Noninvertibility in neural networks," *Computers and Chemical Engineering* **24**, 2417–2433.

Nien, C. H. and Wicklin, F. J. [1998] "An algorithm for the computation of preimages in noninvertible mappings," *Int. J. Bifurcation and Chaos* **8**(2), 415–422.

Osinga, H. M. and England, J. P. [2003] "Global Manifold 1D code, Version 2, software for use with DsTool," `http://www.dynamicalsystems.org/sw/sw/detail?item=27`.

Palis, J. and de Melo, W. [1982] *Geometric Theory of Dynamical Systems*, Springer-Verlag, New York/Berlin.

Wicklin, F. J. [1995] "Pisces: a platform for implicit surfaces and curves and the exploration of singularities," *Technical report GCG #89*, The Geometry Center, University of Minnesota, Minneapolis, MN. Available online at `http://www.geom.uiuc.edu/~fjw/pisces/`.